

## Article

# Hard Evidence from Turtle Shells: Tracing Metal and Non-Metallic Elements Bioaccumulation in Freshwater Ecosystems

Haithem Aib <sup>1,\*</sup>, Badis Bakhouché <sup>2</sup>, Krisztián Nyeste <sup>3,4</sup>, Boglárka Dönczö <sup>5</sup>, Selmane Chabani <sup>2</sup>,  
Amina Saadi <sup>2</sup>, Zsolt Varga <sup>6</sup> and Herta Mária Czédli <sup>6</sup>

- <sup>1</sup> Department of Hydrobiology, Pál Juhász-Nagy Doctoral School of Biology and Environmental Sciences, University of Debrecen, 4032 Debrecen, Hungary
- <sup>2</sup> Laboratory of Biological Oceanography and the Marine Environment (LOBEM), Faculty of Biological Sciences, University of Science and Technology of Houari Boumediene (USTHB), BP 32, Algiers 16111, Algeria; badis\_bakhouché@yahoo.fr (B.B.); chabani.selman@gmail.com (S.C.); amina.saadi\_fsb@usthb.edu.dz (A.S.)
- <sup>3</sup> Department of Hydrobiology, University of Debrecen, 4032 Debrecen, Hungary; nyeste.krisztian@science.unideb.hu
- <sup>4</sup> National Laboratory for Water Science and Water Safety, University of Debrecen, 4032 Debrecen, Hungary
- <sup>5</sup> HUN-REN Institute for Nuclear Research (ATOMKI), 4032 Debrecen, Hungary; donczo.boglarka@atomki.hu
- <sup>6</sup> Department of Civil Engineering, University of Debrecen, 4028 Debrecen, Hungary; vzs@eng.unideb.hu (Z.V.); herta.czedli@eng.unideb.hu (H.M.C.)
- \* Correspondence: haithem.aib@eng.unideb.hu

## Abstract

The longevity, site fidelity, and trophic position of freshwater turtles have led to their increasing recognition as useful bioindicators of environmental contamination. *Mauremys leprosa* ( $n = 25$ ) shells from a Northern African wetland system were examined for trace element concentrations in order to assess shell composition as a non-invasive biomonitoring method. Micro x-ray fluorescence ( $\mu$ XRF) method was used to measure the shell concentrations of 17 elements, including Ca, P, Fe, Zn, Mn, Sr, Pb, Sb, and Al. As would be expected from the structural composition of bony tissues, calcium and phosphorus were the predominant constituents. In addition to bulk concentrations, micro-XRF elemental mapping revealed heterogeneous spatial distributions of essential and toxic elements within the shells, providing visual evidence of bioaccumulation patterns and supporting the use of shells as non-invasive bioindicators. There were statistically significant sex-related differences in the levels of trace elements, with males exhibiting higher concentrations of Mg, Mn, Sb, Pb, and Al ( $p < 0.05$ ). Spearman correlations revealed strong associations between certain shell elements (e.g., Fe, Mn, Ti, Zn) and morphometric parameters. Comparisons with environmental samples (water and sediment) showed moderate to strong correlations, particularly with sediment metal concentrations, supporting the utility of shell chemistry as an integrative exposure matrix. Nonetheless, there were significant percentages of censored or missing values for certain metals (Cu, Ni, and As). This study emphasizes how viable turtle shells are as non-lethal markers of bioaccumulation and stresses how crucial it is to take environmental matrices, element-specific variability, and sex into account when assessing contamination. Longitudinal monitoring, physiological biomarkers, and isotopic analysis should all be used in future studies to bolster the causal relationships between environmental exposure and turtle health.

**Keywords:** *Mauremys leprosa*; freshwater turtles; turtle shell; bioindicator; non-invasive biomonitoring; heavy metals; trace elements



Academic Editors: Claude Fortin and Ana Luísa Patrício da Silva

Received: 21 September 2025

Revised: 27 October 2025

Accepted: 14 November 2025

Published: 18 November 2025

**Citation:** Aib, H.; Bakhouché, B.; Nyeste, K.; Dönczö, B.; Chabani, S.; Saadi, A.; Varga, Z.; Czédli, H.M. Hard Evidence from Turtle Shells: Tracing Metal and Non-Metallic Elements Bioaccumulation in Freshwater Ecosystems. *Environments* **2025**, *12*, 445. <https://doi.org/10.3390/environments12110445>

**Copyright:** © 2025 by the authors. Licensee MDPI, Basel, Switzerland. This article is an open access article distributed under the terms and conditions of the Creative Commons Attribution (CC BY) license (<https://creativecommons.org/licenses/by/4.0/>).

## 1. Introduction

Aquatic ecosystems are vital habitats that support a diverse array of life forms. However, the continuous accumulation of pollutants has placed these ecosystems under significant threat, leading to substantial biodiversity losses [1]. Among these pollutants, heavy metals are of particular concern due to their persistence, toxicity, and detrimental ecological impacts [2,3]. Heavy metals are considered hazardous to both human health and the environment, even at low concentrations [4–6]. While some heavy metals are essential in trace amounts, they become toxic when present in high concentrations [7], with their toxicity depending largely on dosage and exposure duration. Heavy metals are commonly defined as elements with a density greater than  $5 \text{ g}\cdot\text{cm}^{-3}$  (i.e., specific gravity greater than 5) [8]. They are often categorized collectively due to their association with pollution and potential toxicity or eco-toxicity [9]. A more recent refinement to this definition proposes that heavy metals are “naturally occurring metals with an elemental density greater than  $5 \text{ g}\cdot\text{cm}^{-3}$  and an atomic number greater than 20” [10]. Heavy metals such as lead (Pb), cadmium (Cd), chromium (Cr), copper (Cu), nickel (Ni), zinc (Zn), and manganese (Mn) are not readily removed through natural biological processes and are not easily degraded in the environment [11]. Once introduced into aquatic environments, these metals tend to accumulate in sediments and in the tissues of aquatic organisms [12,13]. Their persistence means they can remain in ecosystems for extended periods. Even at low concentrations, heavy metals may exert toxic effects on a wide range of aquatic organisms, including microorganisms, invertebrates, fish, and aquatic plants [14,15]. Ultimately, heavy metal exposure can lead to increased mortality and cause physiological, morphological, or genetic abnormalities, such as reduced growth or developmental disruptions [16–19]. Such disruptions at the organismal level can scale up to affect the stability of entire aquatic ecosystems, altering food web structures and reducing biodiversity [20]. To evaluate the extent of heavy metal accumulation in aquatic biota, several quantitative indices are utilized, including the bio-concentration factor (BCF), bio-accumulation factor (BAF), and bio-accumulation coefficient (BCC). Freshwater ecosystems such as wetlands and lakes are particularly vulnerable because they often act as sinks for pollutants originating from industrial effluents, urban runoff, agricultural activities, and atmospheric deposition [21]. In Algeria, Reghaïa Lake, a Ramsar site located in the northern region—plays a critical ecological role as a biodiversity hotspot and refuge for numerous aquatic and semi-aquatic species. However, the lake’s environmental quality is a concern due to increasing human pressures [22,23]. Reptiles are particularly vulnerable to long-term exposure to contaminants because of their long lifespans and position at the top of the food chain. However, reptiles receive much less attention in ecotoxicological research than animals such as birds and mammals. The Mediterranean pond turtle (*Mauremys leprosa*) is recognized as a species at risk in Algeria [24,25]. A native species found in parts of southern Europe and North Africa, the Mediterranean pond turtle (*Mauremys leprosa*) is an appropriate bioindicator because of its omnivorous diet and habitat fidelity [26] and ability to accumulate contaminants in its tissues over time [27]. Long-term exposure to heavy metals can be evaluated non-invasively using the turtle’s shell, which is primarily made of keratin and bone [28]. Freshwater turtles are a unique group of chelonian fauna [29]. Freshwater turtles are among the vertebrate species that have been shown to serve as biomarkers of environmental contamination, particularly in studies on element pollution [30]. Different turtle species can have different metal levels analyzed. The toxicity level of heavy metals in various tissues of dead specimens can be estimated in threatened and endangered wild species, such as turtles [31]. Given their potential to serve as scavengers in aquatic environments, turtles are known for their many uses. Their longer lifespan enables the tracking of long-term trends in environmental pollutants, and they have enough muscle mass to handle several endpoint measurements [32].

Despite *Mauremys leprosa*'s near threatened status [25], little is known about its ecology and function in Algerian wetland ecosystems. This species can withstand pollution and thrive in degraded habitats, according to numerous studies [27,33]. However, the Réghaïa Ramsar site faces strong anthropogenic pressures from industrial discharge and urban activity, making it essential to evaluate potential metal accumulation in local fauna. However, research conducted at the Ramsar site of Lake Réghaïa has revealed that this species serves as prey for various animal groups within the Réghaïa game reserve [34].

This study offers a pilot non-invasive evaluation of elemental accumulation in *M. leprosa* shells in order to close this knowledge gap. In this study, we aim to evaluate the feasibility of using turtle shells as bioindicator matrices to assess heavy metal contamination while avoiding lethal sampling. By analyzing shell fragments collected from individuals that were naturally predated or scavenged, we also seek to highlight potential trophic transfer risks within freshwater ecosystems.

Accordingly, the objective of this research was to investigate the accumulation of selected heavy metals in the shells of *Mauremys leprosa* collected from Reghaïa Lake. To contextualize these findings, environmental samples of water and sediments were analyzed during both winter and spring to determine spatial and seasonal variations in heavy metal distribution. By comparing environmental concentrations with levels accumulated in the turtle shells, this study enhances understanding of the ecological consequences of heavy metal pollution in Algerian freshwater systems. Furthermore, it underscores the value of non-lethal biomonitoring approaches in ecological assessment and conservation practices.

## 2. Methods and Materials

*Mauremys leprosa* is found in parts of Southern France, the Iberian Peninsula, and North Africa. It is regarded as a “vulnerable” species even though the IUCN Red List lists it as a least concern worldwide [35]. *Mauremys leprosa* is considered an important species for ecotoxicological research due to its key ecological role and its position within aquatic and terrestrial food webs. The species is frequently scavenged by predators such as wolves and wild dogs, meaning that heavy metals accumulated in its tissues through biomagnification can be transferred further up the food chain to terrestrial scavengers. This trophic linkage underscores the potential for contaminants to move across ecosystem boundaries, highlighting *M. leprosa* as a valuable bioindicator for assessing both environmental contamination and its wider ecological implications. Dietary habits in this species change with age; juveniles and subadults primarily consume insects, fish, and mollusks, while adults increasingly shift toward a diet composed of aquatic vegetation and algae [36].

### 2.1. Study Area

The study was conducted at Reghaïa Lake, located in Tipaza province, northern Algeria, Figure 1. The Ramsar Convention recognizes this lake as a protected wetland system, and it provides vital habitat for aquatic animals, such as the native pond turtle (*Mauremys leprosa*), and migratory birds. Anthropogenic pressure on the region is rising as a result of adjacent industrialization, agriculture, and urbanization.

*Mauremys leprosa* is of particular interest in ecotoxicological research due to its ecological role and the fact that it is frequently scavenged by predators such as wolves and wild dogs. When this species accumulates elevated concentrations of heavy metals through biomagnification, these contaminants can subsequently be transferred to terrestrial scavengers, thereby extending the impact of aquatic pollution beyond the aquatic environment. This trophic linkage highlights the species' ecological importance and demonstrates the potential for cross-ecosystem contaminant movement. Consequently, *M. leprosa* serves as

a valuable indicator for assessing environmental contamination and its broader ecological implications.

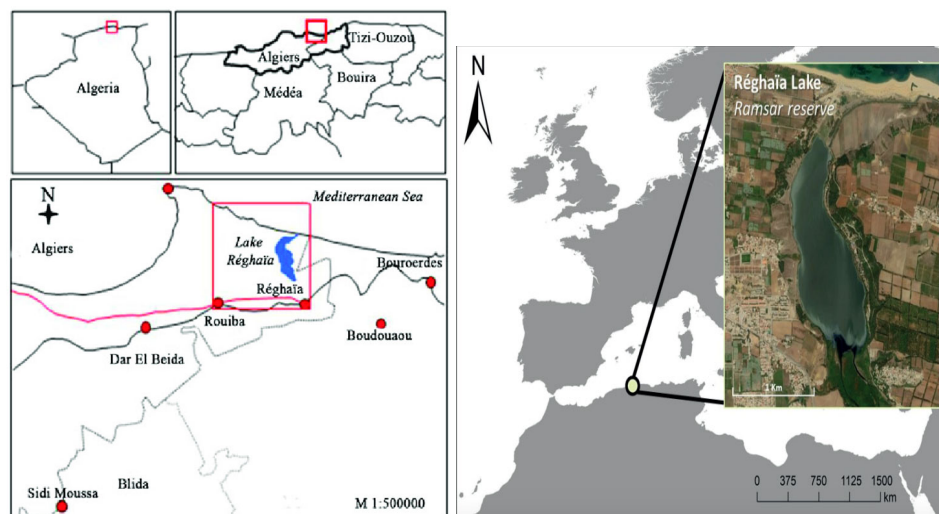


**Figure 1.** Regional context of Lake Reghaïa ( $36^{\circ}45'–36^{\circ}48'$  N,  $3^{\circ}19'–3^{\circ}21'$  E), a 75 ha freshwater Ramsar wetland located 29 km east of Algiers in the Mitidja Plain [37]. The pink box highlights the location of the lake, and the delineated wetland boundary indicates the sampling stations for water, sediment, and turtle shells.

## 2.2. Sample Collection

Samples were gathered in the winter and spring between January and April 2020 at Lake Reghaïa, a Ramsar site that is under a lot of pollution pressure because it is close to a popular tourist beach. Water samples (20 cm below the surface) and surface sediments (~5 cm depth) were collected from different locations around the lake to evaluate seasonal changes in heavy metal concentrations. In addition, about thirty *Mauremys leprosa* shell samples were obtained primarily from individuals that had been scavenged or predated, as well as from naturally shed scutes and remains found in proximity to the lake. All biological sampling procedures were conducted in accordance with strict ethical guidelines. Given the ecological importance of the lake and the increasing anthropogenic pressures in the surrounding area, these turtle shells provide a valuable non-lethal bioindicator for assessing contamination levels of both metallic and non-metallic elements within the ecosystem.

## 2.3. Environmental Sampling, Preservation, and Acid Digestion

Water samples were collected in pre-cleaned, acid-washed polyethylene bottles (500 mL). Where total recoverable metals were targeted, samples were collected unfiltered and acidified in the field to pH < 2 with ultrapure concentrated HNO<sub>3</sub> (trace-metal grade). The volume of acid added and the final pH were recorded for each bottle. Samples were stored at 4 °C and transported to the laboratory within 12 h. Field blanks (bottles filled with ultrapure water opened at the site and handled identically) were collected during each campaign.

Surface sediments (0–5 cm) were collected using a stainless-steel grab/corer and transferred to pre-cleaned polyethylene bags. Samples were kept cool in the field and transported to the laboratory on ice. In the laboratory, sediment samples were homogenized, stones and coarse debris were removed, air-dried at  $\leq 40$  °C, sieved to <2 mm, and stored in sealed containers prior to analysis. Dry mass and moisture content were determined for each sample for concentration normalization to dry weight.

Aliquots of 50–100 mL of each acidified water sample were transferred to digestion vessels and treated with 5 mL of concentrated HNO<sub>3</sub>. Sediment aliquots (0.2–0.5 g dry

weight) were digested following EPA 3051A (microwave-assisted  $\text{HNO}_3 \pm \text{HCl}$ ) or EPA 3050B ( $\text{HNO}_3 + \text{H}_2\text{O}_2$  followed by  $\text{HCl}$ ) protocols. Briefly, weighed sediment aliquots were placed in Teflon/microwave vessels and treated with concentrated  $\text{HNO}_3$ . In addition, subjected to the microwave program recommended for the instrument (ramp and hold temperatures per manufacturer and EPA 3051A protocol).

#### 2.4. Turtle Shell Preparation and Analysis

Collected turtle shells were first cleaned of debris, rinsed with deionized water, and air-dried.

##### 2.4.1. Shell Morphometric Analysis

Morphometric measurements were conducted to assess the physical dimensions of the turtle shells. Table 1 presents the morphometric data, including the straight-line carapace. The samples were categorized by sex for analysis.

**Table 1.** Morphometric parameters of turtle shells.

n	Sex	LA (mm)	Lp (mm)	L
1	M	124.4	NA	NA
2	M	110.1	NA	NA
3	M	83	NA	NA
4	F	96	NA	NA
5	M	116.1	134	193
6	M	139.2	158.1	200
7	M	111	NA	189
8	M	127	131	195
9	M	116	132	199
10	F	126	NA	NA
11	M	115	129	193
12	M	112	126	189
13	M	112	130	189
14	F	124	144	207
15	M	112	128	186
16	F	NA	149	NA
17	F	NA	121	NA
18	F	118	129	195.5
19	F	122.9	134.9	187
20	F	114.2	126	195.5
21	F	111	NA	NA
22	F	110	128	184
23	F	111	124	179
24	F	122	144	216
25	F	118.9	140	207.5

NA = Not Available; measurements were not recorded for these individuals due to damage. LA: maximum shell length; Lp: effective length; L: overall shell length.

##### 2.4.2. Analytical Techniques

Micro-XRF mapping measurements were carried out using a Bruker M4 TORNADO (Bruker, Billerica, MA, USA) instrument with an Rh-tube X-ray source without any filter at 50 kV accelerating voltage and 400  $\mu\text{A}$  current. The mapping was performed in a 20 mbar vacuum on an approximately 1  $\text{cm}^2$  area of the flat surface of each sample. The spot size of the beam was focused to 20  $\mu\text{m}$  by the built-in polycapillary lens, and the step size of the mapping was 40  $\mu\text{m}$  with 1 mm/s velocity. Characteristic X-ray lines were collected and recorded by two energy dispersive detectors, each with a 30  $\text{mm}^2$  active area. X-ray lines of hydrogen, carbon, nitrogen, and oxygen cannot be detected with the instrument, so the

measurements are considered to be semi-quantitative. The evaluation was performed by the M-Quant built-in software (version 1.6.621.0) of the M4 TORNADO with the fundamental parameter (FP) approach. Spectrometer calibration was checked before measurements using the certified Bruker standards plate (4110-7512-000; SN: 0262; Bruker, Billerica, MA, USA). Additional certified standards were used as self-checks: FM007237 (RM PR24 FX 707—Gold jewellery alloy for micro-XRF, Fluxana, Bedburg-Hau, Germany, 2016); FM007274 (RM PR24 FX 744—Gold jewellery alloy for micro-XRF, Fluxana, Bedburg-Hau, Germany, 2016); 133X AGA3 A (Archaeological silver, ARMI MBH, Manchester, NH, USA, 2014); 133X AGA2 A (Silver alloy, ARMI MBH, Manchester, NH, USA, 2020); IARM 90C (certificate no. 90C-11302011-IARM-F, ARMI MBH, Manchester, NH, USA, 2011); MBH 31X78735.8 B (Leaded brass, ARMI MBH, Manchester, NH, USA, 2016); and MBH 32X SN6 B (Bronze, ARMI MBH, Manchester, NH, USA, 2018).

Atomic Absorption Spectrometry (AAS) performed metal determinations using a Varian AA-240FS (Varian Australia Pty Ltd., Mulgrave, Victoria, Australia) equipped with Zeeman background correction. Routine analyses were performed with flame AAS using an air-acetylene flame. For low-level determination of Cd and Pb, a graphite furnace AAS (GF-AAS) was used. Analytical wavelengths (nm) used were Cd 228.8; Cr 357.9; Cu 324.8; Mn 279.5; Ni 232.0; Pb 217.0; and Zn 213.9. Instrument operational parameters (lamp currents, slit widths, burner height, and flow rates) and the GF-AAS furnace temperature program (drying, pyrolysis, atomization, and cleanout temperatures and hold times) were optimized according to the instrument's standard operating procedures. Each sample was measured in triplicate; the reported value is the mean of replicate readings after passing QC checks.

### 2.5. Quality Assurance and Quality Control (QA/QC)

Strict quality assurance and control procedures were applied to all  $\mu$ XRF measurements to guarantee accurate results. Calibration was confirmed using certified reference materials as mentioned above. Relative standard deviation (RSD) was consistently less than 5%.

Element-specific limits of detection (LOD) were determined based on the publication of Rousseau [38] and are reported in ppm ( $\equiv$ mg·kg<sup>-1</sup>):

Mg 116; P 13; S 4; K 2; Ca 6; Ti 6; Mn 2; Fe 4; Zn 3; Sr 4; Al 41; Sb 67; Cu 2; Pb 1; Ni 1; Si 14; As 1 ppm.

Adequate analytical sensitivity for the majority of trace and macro-elements is confirmed by the LOD values, which fall within the range usually obtained for energy-dispersive  $\mu$ XRF analyses of biogenic calcified tissues like bone and shell. These QA/QC procedures ensure data precision, reproducibility, and comparability with other ecotoxicological studies of chelonian shell materials.

### 2.6. Data Analysis

All statistical analyses were conducted using Python v3.11. To determine the suitability of statistical methods, data distributions were assessed for normality using Shapiro–Wilk, D'Agostino–Pearson, Jarque–Bera, and Anderson–Darling tests. Variables meeting assumptions of normality (P, S, Ca, Sb) were analyzed using parametric tests (independent *t*-test for two-group comparisons; one-way ANOVA for multiple groups). Non-normally distributed variables (Mg, K, Ti, Mn, Fe, Zn, Sr, Al, Si) were evaluated with non-parametric alternatives (Mann–Whitney U test and Kruskal–Wallis test). Metals with >30% missing values (Cu, Pb, Ni, As) were excluded from inferential tests. Descriptive statistics (mean  $\pm$  standard deviation) were calculated for morphometric parameters and shell element concentrations, and sex-based differences were tested. Correlation analyses between shell elements, morphometrics, and sex were performed using Spearman rank correlation. To explore relationships between turtle shell chemistry and environmental compartments (sediment and water),

element-specific Spearman correlations were computed across seasonal datasets. All statistical tests were two-tailed, and significance was set at  $p \leq 0.05$ . Graphical outputs (heatmaps, bar charts, and network diagrams) were generated.

### 2.7. Shell–Environment Correlations and Multiple Testing Correction

Correlations between average site-level shell concentrations and corresponding environmental matrices (sediment and water, winter and spring) were assessed using Spearman’s rank correlation ( $\rho$ ). Because four independent comparisons were performed,  $p$ -values were corrected for multiple testing using the Benjamini–Hochberg false discovery rate (FDR) procedure [39] to reduce the likelihood of false positives. Both raw and FDR-adjusted  $p$ -values are presented and statistical significance was accepted at  $\alpha = 0.05$  after correction. All calculations were performed using the *p.adjust()* function in R (method = “BH”).

## 3. Results

### 3.1. Morphometric Parameters

Table 2 presents descriptive statistics for morphometric measurements of *Mauremys leprosa*. No significant differences were observed between males and females in maximum shell length (LA), axial length, or effective length (Lp) ( $p > 0.05$ ).

**Table 2.** Descriptive statistics (mean  $\pm$  SD) of morphometric parameters in *Mauremys leprosa*.

Variable	Overall (mm)	Male (mm)	Female (mm)
LA	115 $\pm$ 11	115 $\pm$ 13	116.1 $\pm$ 8.0
Axial length	134.1 $\pm$ 9.3	133.5 $\pm$ 9.6	134.5 $\pm$ 9.0
Lp	195.1 $\pm$ 9.4	192.6 $\pm$ 4.5	198 $\pm$ 12

### 3.2. Elemental Composition

Table 3 presents the elemental concentrations in turtle shells. Calcium and phosphorus were the predominant components, reflecting the structural composition of bone and keratin. Trace elements such as Fe, Zn, Mn, and Sr were also detected at lower but notable levels. All reported elemental concentrations were above the instrument-specific limits of detection, except where indicated as BDL (Below Detection Limit). The element-specific LODs ranged from 1 ppm (Pb, Ni, As) to 116 ppm (Mg), confirming that the  $\mu$ XRF system provided adequate sensitivity for detecting both major (Ca, P) and trace constituents in the turtle shell matrix.

**Table 3.** Elemental concentrations ( $\text{mg kg}^{-1}$ ) in *Mauremys leprosa* shells.

Element	Overall	Male	Female	Test	$p$ -Value	Sig.
<b>Non-normally distributed elements</b>						
Mg	3622 (3184–4105)	4026 (3550–4460)	3275 (2900–3600)	Mann–Whitney U	0.04	*
K	1096 (820–1370)	1268 (970–1600)	952 (700–1150)	Mann–Whitney U	0.07	n.s.
Ti	346 (190–470)	389 (210–540)	307 (180–410)	Mann–Whitney U	0.29	n.s.
Mn	195 (85–310)	277 (130–420)	122 (55–210)	Mann–Whitney U	0.05	*
Fe	2151 (950–3200)	2397 (1200–3650)	1942 (800–2800)	Mann–Whitney U	0.31	n.s.
Zn	598 (410–760)	632 (450–780)	569 (400–730)	Mann–Whitney U	0.42	n.s.
Sr	1622 (1200–2050)	1690 (1300–2200)	1560 (1100–1900)	Mann–Whitney U	0.66	n.s.
Al	3975 (2300–5200)	4813 (3100–6100)	3216 (1900–4100)	Mann–Whitney U	0.03	*
Si	8943 (5100–12,400)	11,06 (6800–15,000)	6938 (4200–9400)	Mann–Whitney U	0.06	n.s.

Table 3. Cont.

Element	Overall	Male	Female	Test	p-Value	Sig.
<b>Normally distributed elements</b>						
<b>P</b>	101,461 ± 11,594.13	100,015 ± 11,916	102,700 ± 11,163	<i>t</i> -test	0.55	n.s.
<b>S</b>	3126 ± 1160	3493 ± 1230	2806 ± 961	<i>t</i> -test	0.09	n.s.
<b>Ca</b>	415,698 ± 17,697	414,450 ± 18,059	416,799 ± 17,607	<i>t</i> -test	0.48	n.s.
<b>Sb</b>	1491 ± 1082	2109 ± 1156	904 ± 704	<i>t</i> -test	0.02	*
<b>Cu</b>	4.6 ± 9.7	7.3 ± 12.4	2.3 ± 6.4	Mann–Whitney U	0.08	n.s.
<b>Pb</b>	9.6 ± 20.4	14.3 ± 24.3	5.4 ± 15.8	Mann–Whitney U	0.04	*
<b>Ni</b>	0.23 ± 0.78	0.00 ± 0.00	0.42 ± 0.99	Mann–Whitney U	0.15	n.s.
<b>As</b>	Excluded (>30% missing)	—	—	—	—	—

Note: Data distributions were tested for normality using the Shapiro–Wilk test. Non-normally distributed variables (Mg, K, Ti, Mn, Fe, Zn, Sr, Al, Si) are presented as median (interquartile range), while normally distributed variables are expressed as mean ± standard deviation (SD). All values are reported to two decimal places. “n.s.” = not significant; “\*” =  $p < 0.05$ ; element-specific LODs (ppm): Mg 116, P 13, S 4, K 2, Ca 6, Ti 6, Mn 2, Fe 4, Zn 3, Sr 4, Al 41, Sb 67, Cu 2, Pb 1, Ni 1, Si 14, As 1.

### 3.3. Sex-Based Differences

Significant differences were observed between sexes; males accumulated higher concentrations of Mg, Mn, Sb, and Pb, whereas females showed elevated Al levels ( $p < 0.05$ ). Normality testing indicated that P, S, Ca, and Sb followed normal distributions, while the remaining elements displayed skewed patterns. Accordingly, parametric tests were applied to normally distributed elements, and non-parametric tests were used for the others.

### 3.4. Micro-XRF Elemental Mapping

The distributions of major and trace elements in the 25 turtle shell samples were found to be heterogeneous by micro-XRF elemental mapping (Figure 2). In accordance with the structural composition of keratinized bone tissue, calcium and phosphorus were consistently the most prevalent elements, forming a homogeneous matrix. Trace elements like Fe, Zn, Mn, and Sr showed up as localized hotspots, frequently centered along the shell’s microstructural features and growth lines. Conversely, elements that could be harmful, such as Pb, Sb, and Al, displayed unequal and irregular deposition, with higher intensities in certain individuals, indicating varying exposure to the environment. These maps show that the distribution of elemental accumulation is not uniform; rather, it reflects the microstructure of the shell as well as the sources of external contamination.

### 3.5. Correlation Patterns Among Shell Elements

Correlations among morphometric parameters and elemental concentrations in *Mauromys leprosa* shells are presented in Table 4 and visualized in Figure 3. Overall, several moderate to strong positive associations were observed among shell elements. Notably, Ti showed very strong correlations with Fe ( $\rho = 0.986$ ) and Al ( $\rho = 0.977$ ), while K was positively associated with S ( $\rho = 0.655$ ), P ( $\rho = 0.699$ ), and Zn ( $\rho = 0.754$ ). Other notable relationships included Mg–Si ( $\rho = 0.591$ ), Cu–Pb ( $\rho = 0.664$ ), and Ti–Si ( $\rho = 0.977$ ). In contrast, most morphometric variables, including axial length (Axial), plastron length (Lp), and shell length (L), exhibited weak or non-significant correlations with elemental concentrations. Some exceptions were observed for sex, which correlated moderately with K ( $\rho = 0.500$ ), Ca ( $\rho = 0.511$ ), Mn ( $\rho = 0.489$ ), Al ( $\rho = 0.455$ ), Sb ( $\rho = -0.611$ ), Cu ( $\rho = 0.563$ ), and Si ( $\rho = 0.411$ ). All correlation coefficients were calculated using Spearman’s rank method on the final validated dataset ( $n = 25$ ), and  $p$ -values were corrected for multiple comparisons using

the Benjamini–Hochberg false discovery rate (FDR) procedure. Following this adjustment, only a few associations remained statistically significant, confirming that the observed correlations reflect robust relationships rather than chance effects. The numerical results in Table 4 are fully consistent with the graphical representation in Figure 3.

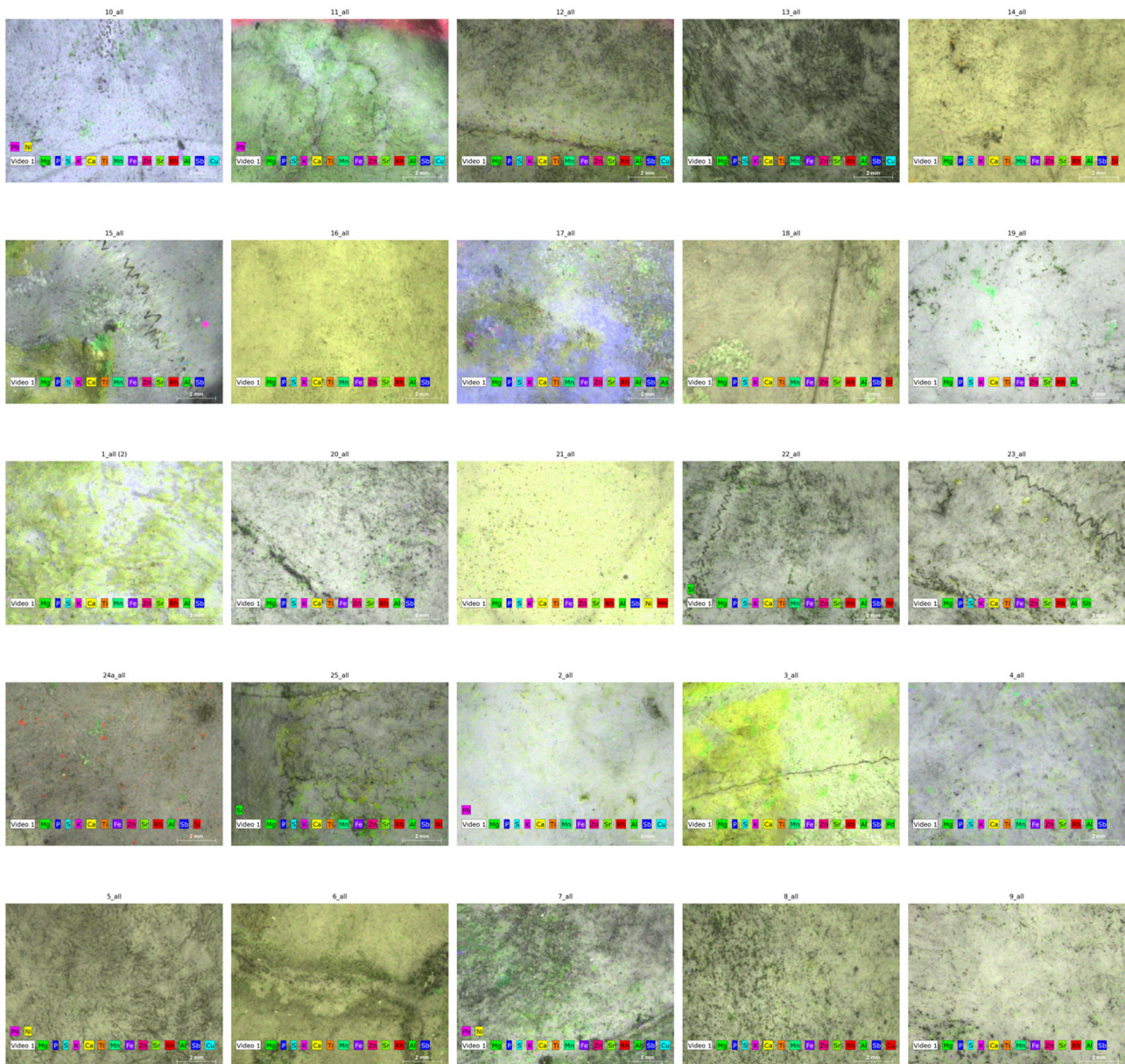


**Figure 2.** Elemental distribution maps obtained using  $\mu$ XRF. The white box contains the Video 1 title, which means the camera image. Colorful boxes refer to the detected elements on the surface of a fish scale. Micro-XRF elemental distribution maps of *Mauremys leprosa* shells. The distributions of major and trace elements in the 25 turtle shell samples were heterogeneous, as revealed by micro-XRF mapping. Calcium and phosphorus formed a homogeneous matrix consistent with the structure of keratinized bone tissue. Trace elements such as Fe, Zn, Mn, and Sr appeared as localized hotspots aligned with microstructural features and growth lines. Potentially harmful elements (Pb, Sb, Al) showed irregular and uneven deposition patterns, with elevated intensities in certain individuals, indicating variable environmental exposure.

**Table 4.** Spearman’s rank correlation coefficients ( $\rho$ ) among morphometric parameters and elemental concentrations in *Mauremys leprosa* shells. Correlation coefficients were calculated using the final validated dataset ( $n = 25$ ).  $p$ -values were adjusted for multiple testing using the Benjamini–Hochberg false discovery rate (FDR) procedure. Non-significant correlations ( $p > 0.05$ , FDR-adjusted) are indicated as “N.S.” Results are fully consistent with those shown in Figure 3.

	Sex	LA	Axial	Lp	L	Mg	P	S	K	Ca	Ti	Mn	Fe	Zn	Sr	Al	Sb	Cu	Pb	Ni	Si	As
Sex	1.000	N.S.	N.S.	N.S.	N.S.	N.S.	N.S.	0.500	0.511	N.S.	N.S.	0.489	N.S.	0.422	−0.611	0.455	0.311	0.563	N.S.	N.S.	0.411	N.S.
LA		1.000	0.834	0.707	N.S.	N.S.	N.S.	N.S.	N.S.	N.S.	N.S.	N.S.	N.S.	N.S.	N.S.	N.S.	−0.438	N.S.	N.S.	N.S.	N.S.	N.S.
Axial			1.000	0.704	N.S.	N.S.	N.S.	N.S.	N.S.	N.S.	N.S.	N.S.	N.S.	N.S.	N.S.	N.S.	N.S.	N.S.	N.S.	N.S.	N.S.	N.S.
Lp				1.000	N.S.	N.S.	N.S.	N.S.	N.S.	N.S.	N.S.	N.S.	N.S.	N.S.	N.S.	N.S.	N.S.	N.S.	N.S.	N.S.	N.S.	N.S.
L					1.000	N.S.	N.S.	N.S.	N.S.	N.S.	N.S.	N.S.	N.S.	N.S.	N.S.	N.S.	N.S.	N.S.	N.S.	N.S.	N.S.	N.S.
Mg						1.000	N.S.	N.S.	N.S.	0.505	N.S.	N.S.	N.S.	N.S.	N.S.	N.S.	N.S.	0.591	N.S.	N.S.	N.S.	N.S.
P							1.000	−0.723	−0.438	0.699	N.S.	−0.440	N.S.	N.S.	N.S.	N.S.	N.S.	N.S.	N.S.	N.S.	N.S.	N.S.
S								1.000	0.602	N.S.	N.S.	0.655	N.S.	N.S.	N.S.	N.S.	N.S.	N.S.	N.S.	N.S.	N.S.	N.S.
K									1.000	N.S.	0.804	0.754	0.815	N.S.	N.S.	0.881	N.S.	0.455	N.S.	N.S.	0.852	N.S.
Ca										1.000	N.S.	N.S.	N.S.	N.S.	N.S.	N.S.	N.S.	N.S.	N.S.	N.S.	N.S.	N.S.
Ti											1.000	0.703	0.986	N.S.	N.S.	0.957	N.S.	N.S.	N.S.	N.S.	0.977	N.S.
Mn												1.000	0.701	N.S.	N.S.	0.744	N.S.	N.S.	N.S.	N.S.	0.733	N.S.
Fe													1.000	N.S.	N.S.	0.951	N.S.	N.S.	N.S.	N.S.	0.961	N.S.
Zn														1.000	N.S.	N.S.	0.364	N.S.	N.S.	N.S.	N.S.	N.S.
Sr															1.000	N.S.	N.S.	N.S.	N.S.	N.S.	N.S.	N.S.
Al																1.000	N.S.	N.S.	N.S.	N.S.	0.991	N.S.
Sb																	1.000	N.S.	N.S.	N.S.	N.S.	N.S.
Cu																		1.000	0.664	N.S.	N.S.	N.S.
Pb																			1.000	N.S.	N.S.	N.S.
Ni																				1.000	N.S.	N.S.
Si																					1.000	N.S.
As																						1.000

Only significant correlations are shown ( $p \leq 0.05$ ); non-significant values are indicated as N.S. Sex is coded as female = 0, male = 1. Morphometric parameters: LA—maximum shell length (mm); Axial length—maximum straight-line carapace length (mm); Lp—effective length (mm); L—overall length (mm).

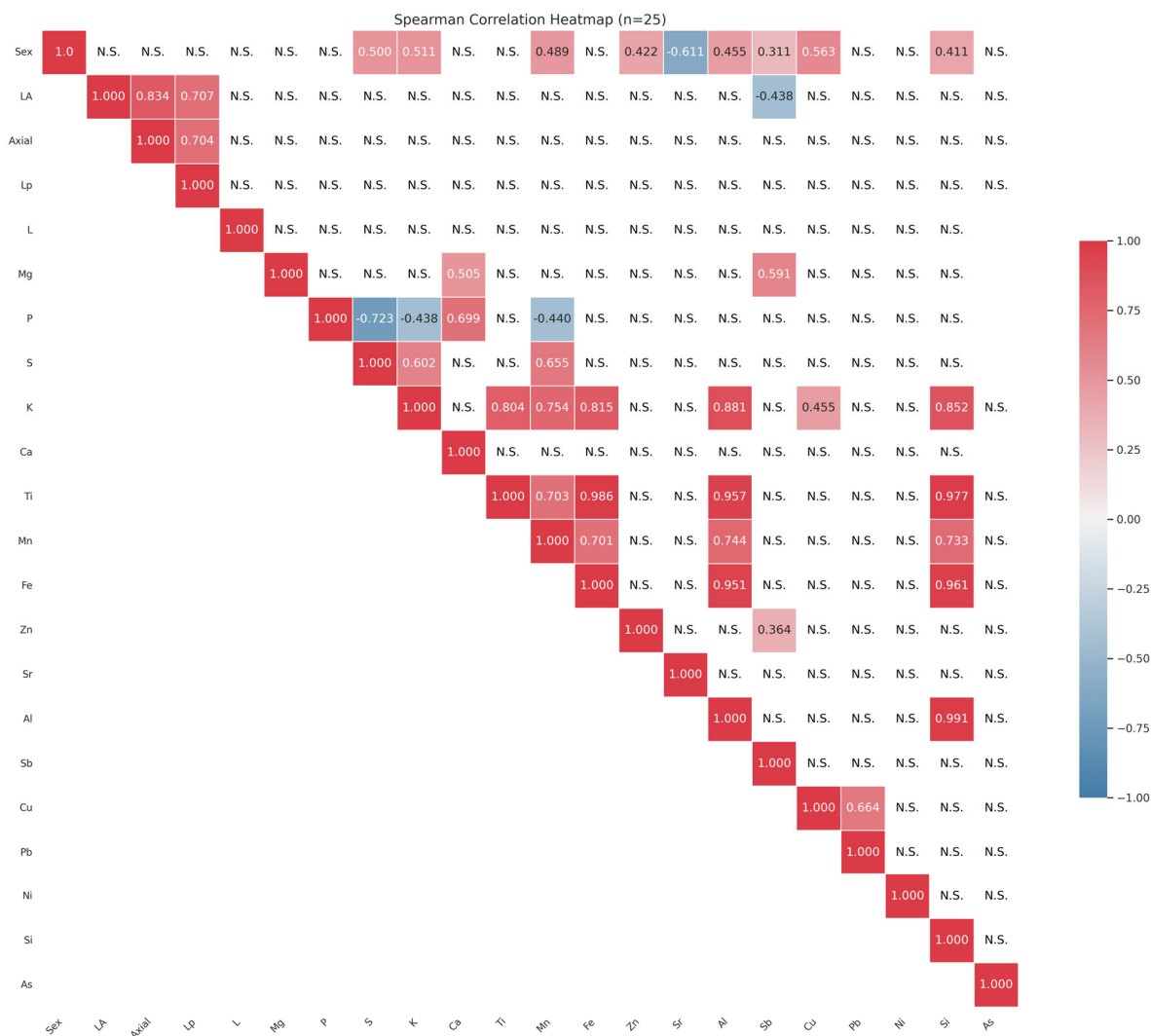


**Figure 3.** Spearman’s rank correlation matrix of elemental concentrations and morphometric variables in *Mauremys leprosa* shells (final dataset, n = 25). Color intensity indicates the strength and direction of  $\rho$ . Non-significant correlations ( $p > 0.05$ , FDR-adjusted) are marked as “N.S.”. Correlation matrix of morphometric parameters and elemental concentrations. Pairwise Spearman’s rank correlation coefficients (n = 25) are shown for all morphometric and elemental variables.  $p$ -values were adjusted for multiple comparisons using the Benjamini–Hochberg false discovery rate (FDR) procedure. Only correlations that remained statistically significant after FDR correction are marked. This figure complements the numerical results presented in Table 4.

3.6. Seasonal Variation in Heavy Metals in Sediments and Water

The concentrations of selected metals in sediments and water are presented in Table 5. Sediments contained higher levels of Cu, Mn, Ni, Pb, and Zn compared to water, where most metals were detected at trace or non-detectable levels. Seasonal variation was evident, with sediment Cu decreasing from winter (37.51 mg/kg) to spring (10.55 mg/kg), while Zn increased from 12.14 to 25.58 mg/kg.

**Table 5.** Seasonal variation in heavy metal concentrations in sediments and water samples.

		Cadmium	Chromium	Copper	Manganese	Nickel	Lead	Zinc
Sediments (mg/kg)	Winter	0	0	37.51	95.47	72.04	8.73	12.14
	spring	0	0	10.55	83.79	12.33	6.26	25.58
Water (mg/L)	Winter	0	0	0.04	0.07	0.04	0	0
	spring	0	0	0	0.03	0.02	0.04	0

### 3.7. Bioindicator Relationships Between Shell and Environmental Concentrations

A comparison of average metal concentrations across shells, sediments, and water is shown in Figure 4. Shells consistently reflected higher long-term accumulation of trace metals (e.g., Zn, Mn, Pb) compared to water, with sediment values lying in between.

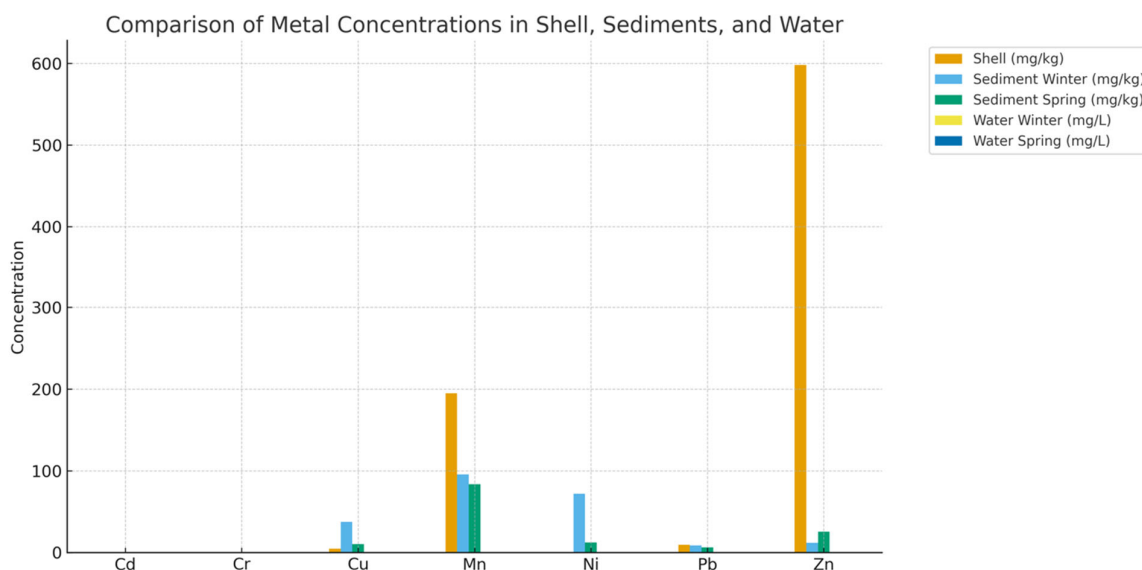


**Figure 4.** Bar chart comparing average element concentrations in turtle shells, sediments (winter and spring), and water (winter and spring).

While all other comparisons were weak ( $|\rho|$ ). Spearman rank correlations showed a moderately positive association between shell and sediment element concentrations in spring ( $\rho = 0.50, p = 0.391$ ;  $<0.30, p > 0.6$ ; Table 6). Using the Benjamini–Hochberg false discovery rate (FDR) procedure to account for multiple comparisons, none of the relationships were still statistically significant (FDR-adjusted  $p > 0.05$ ). The direction and magnitude of the coefficients. Especially the moderate correlation with sediments implies that turtle shells and sediments may record similar long-term exposure signals. while water concentrations capture more short-term variability, even though these results were not significant.

Table 6 summarizes the correlation coefficients ( $\rho$ ), raw  $p$ -values, and FDR-adjusted  $p$ -values for the four environmental comparisons.

**Table 6.** Spearman rank correlations ( $\rho$ ) between shell element concentrations and environmental matrices (sediment and water) for two sampling seasons.  $p$ -values were corrected for multiple testing using the Benjamini–Hochberg false discovery rate (FDR) procedure; none of the correlations remained significant after correction (FDR-adjusted  $p > 0.05$ ).

Comparison	Spearman’s Rho	$p$ -Value	FDR-Adjusted $p$
Sediment Winter	−0.20	0.747	1.00
Sediment Spring	0.50	0.391	1.00
Water Winter	−0.26	0.668	1.00
Water Spring	−0.05	0.935	0.94

## 4. Discussion

### 4.1. Elemental Composition of Turtle Shells

The predominance of calcium and phosphorus in *Mauremys leprosa* shells underscores their essential structural role in the mineralized matrices of bone and keratin [40–42]. This finding aligns with previous studies on chelonians and other vertebrates, where

skeletal integrity and shell rigidity are attributed to calcium–phosphorus (Ca–P) complexes [43]. These macronutrients are vital for egg formation, skeletal maintenance, and shell strength [44–46]. In addition to Ca and P, trace metals such as iron (Fe), zinc (Zn), manganese (Mn), and strontium (Sr) were also detected, likely reflecting their physiological functions in mineral substitution, enzymatic activity, and bone metabolism [43]. The presence of non-essential or potentially toxic elements, including aluminum (Al), antimony (Sb), and lead (Pb), suggests environmental contamination, reinforcing the role of the shell as a passive reservoir for exogenous pollutants. Similar patterns have been observed in other keratinous structures such as fish scales, bird feathers, and reptilian skin, further supporting the shell's function as a sink for environmental contaminants [43,47].

#### 4.2. Sex-Based Differences in Metal Accumulation

Sexual dimorphism in trace element accumulation was evident, with males exhibiting higher Mg, Mn, Sb, and Pb, while females showed elevated Al levels. Such differences may arise from a combination of behavioral and physiological factors [48,49]. Male tortoises often display greater mobility and wider home ranges, increasing exposure to contaminated microhabitats [50,51]. Additionally, differences in metabolic rate and calcium mobilization for egg production in females could influence element partitioning, with excess metals being sequestered differently between the sexes [52–54]. Elevated Pb and Sb in males are particularly concerning, as both elements are strongly linked to anthropogenic sources such as vehicular emissions, industrial discharge, and contaminated soils [43,55]. Comparable patterns of lead enrichment have been reported in freshwater turtles inhabiting urban and industrially impacted wetlands, where males accumulated higher concentrations due to wider home ranges and increased environmental contact [43]. The presence of Sb, although less frequently studied in reptiles, has also been associated with industrial activities and may act synergistically with Pb to exacerbate toxic effects [47]. In contrast, higher Al concentrations in females may reflect differences in dietary intake or sex-dependent detoxification pathways. Since the majority of pet aquatic and semi-aquatic turtles are omnivores, fresh vegetable products and fresh animal protein sources should make up the majority of their diet. Depending on the species of turtle, the amount and kind of protein sources will change [56]. In contrast to males, females employ a variety of detoxifying strategies, including ones that are energy-intensive, to preserve reproductive fitness and safeguard their genetic material when exposed to higher levels of heavy metal and organic compound pollution [57,58]. Similar sex-related differences in trace element burdens have been observed in other chelonian species, where reproductive demands and calcium mobilization influenced the partitioning of metals [55]. Taken together, our results are consistent with previous evidence and reinforce the necessity of considering sex as a biological variable when evaluating turtles as bioindicators of elemental contamination. More territorial mobility, higher metabolic activity, and dietary or foraging range differences from females, which frequently decrease activity during reproductive periods, are some examples of sex-specific physiological or behavioral differences that may influence exposure and accumulation, as well as the higher aluminum (Al) concentrations seen in males [59].

#### 4.3. Elemental Mapping

The micro-XRF elemental maps provide spatially resolved confirmation of the compositional trends observed in the bulk analyses. The relatively homogeneous distributions of calcium and phosphorus are consistent with their established roles in the mineralization of turtle shells, as widely documented in studies of chelonian hard tissues (e.g., blood, scutes, and shell chemistry) [60,61]. In contrast, the distributions of environmentally derived metals, including Fe, Zn, and Mn, exhibit localized hotspot-like patterns. These patterns

resemble those reported in other keratinous and calcified tissues, where environmentally sourced elements are deposited heterogeneously rather than structurally [61,62].

Notably, the patchy localization of Pb and Sb in certain individuals aligns with previous findings that documented spatially variable lead accumulation in the shells and scutes of turtles inhabiting contaminated or urbanized areas. Such variability is indicative of episodic or point-source contamination rather than uniform chronic exposure [55,62]. The sex-dependent differences observed in our dataset—higher Pb and Sb concentrations in males and higher Al concentrations in females—may reflect distinctions in foraging behavior, habitat use, or physiological processes such as maternal transfer during vitellogenesis. These patterns are consistent with earlier research reporting sex-specific variation in metal burdens in *Mauremys* species and other freshwater turtles [60,61]. Together, these results demonstrate the complementary value of combining micro-XRF imaging with bulk chemical assays. While bulk measurements provide quantitative concentration data suitable for statistical evaluation, micro-XRF adds spatial context, distinguishing structural components of the shell from environmentally derived elemental deposition. Increasingly, methodological reviews of X-ray fluorescence imaging in biological tissues recommend such integrative analytical approaches [63].

Overall, the observed spatial heterogeneity and sex-linked variation support the suitability of freshwater turtle shells, particularly *Mauremys leprosa*, as effective non-invasive bioindicators of trace element contamination. However, the findings also underscore the importance of accounting for biological factors such as sex, age, growth stage, and scute deposition history when interpreting exposure signals.

#### 4.4. Relationships with Morphometrics

Significant correlations between shell morphometric parameters and elemental concentrations indicate that growth influences bioaccumulation in *Mauremys leprosa*. Individuals with larger or longer shells tended to exhibit higher concentrations of certain metals, which is consistent with the cumulative nature of contaminant integration over time. These findings support the use of shell chemistry as a non-invasive, long-term biomarker of environmental exposure and habitat quality. However, not all morphometric traits were strongly associated with elemental burdens, suggesting that metal incorporation is not driven solely by growth. External factors such as diet, habitat conditions, trophic interactions, and seasonal fluctuations likely also influence trace element uptake. This combined influence highlights the importance of interpreting bioaccumulation patterns within a framework that considers both organismal biology and environmental context.

#### 4.5. Environmental Correlations and Bioindicator Potential

The positive correlations observed between metal concentrations in turtle shells and those in surrounding sediments and water highlight the strong potential of shells as reliable bioindicators of local contamination. In particular, elements such as Fe, Mn, and Zn exhibited consistent relationships with environmental matrices, reflecting patterns previously reported in other calcified bioindicator tissues such as fish scales and mollusk shells [64,65]. Because turtles are long-lived, relatively sedentary, and exposed to both aquatic and terrestrial inputs, their shells integrate contaminant exposure over extended times. The correspondence between heavy metal levels in shell tissues and those measured in water and sediments reinforces the value of *Mauremys leprosa* as a sentinel species for monitoring ecosystem health and detecting chronic pollution [64,66].

Following FDR correction, the lack of statistically significant correlations is probably due to the small sample size ( $n = 25$ ) and restricted temporal and spatial coverage, which lower statistical power rather than ecological association. However, the moderate

correlation ( $\rho = 0.50$ ) between shell and sediment metal levels shows a consistent pattern of co-variation consistent with biological expectations. Given their slow mineralization and metabolic inertness, turtle shells accumulate trace elements over similar time scales to sediments, which serve as long-term sinks for particulate-bound metals. Conversely, water concentrations have weaker associations because they are frequently ephemeral and affected by episodic inputs.

Stronger correlations are found under larger sampling designs, and shell and blood metal levels reflect local sediment contamination, according to similar studies on *Mauremys leprosa* and other freshwater turtles (e.g., [60,67]). Future research integrating tissue validation and expanded spatial–temporal coverage would therefore strengthen the causal interpretation between environmental exposure and shell bioaccumulation.

#### 4.6. Ecological and Conservation Implications

The accumulation of toxic metals such as lead (Pb) and antimony (Sb) carries significant ecological implications for chelonians. Lead, in particular, is known to disrupt calcium metabolism, impair immune function, and contribute to pathological conditions such as shell disease in emydid turtles [55,68]. These effects are especially concerning given the long lifespan and slow detoxification rates of turtles, which make them vulnerable to chronic exposure and bioaccumulation. The presence of Pb and Sb in shell tissue not only reflects environmental contamination but also signals potential health risks to individual organisms and broader ecosystem integrity [55,69–71]).

While sequestration of Pb in the shell may reduce systemic toxicity, it signals persistent environmental exposure with potential long-term consequences for health and reproduction [72,73]. Sb, although less studied in reptiles, is linked to industrial emissions and may act synergistically with other metals to exacerbate oxidative stress [72,74,75].

The presence of heavy metals in the shells of the Mediterranean pond turtle (*Mauremys leprosa*) serves as an early warning signal of ecosystem degradation. This species inhabits Mediterranean wetlands that are increasingly threatened by pollution from agricultural runoffs and industrial effluents, and urban expansion. *M. leprosa* bioaccumulates these metals in its tissues, making it a reliable bioindicator of water quality and environmental stress—even under conditions where individuals may appear physiologically healthy. According to [27,60], elevated concentrations of metals such as lead (Pb), zinc (Zn), and copper (Cu) in *M. leprosa* reflect contamination from surrounding aquatic environments, reinforcing its value as a sentinel species for monitoring ecosystem health.

## 5. Conclusions

This study provides new insights into the elemental composition of *Mauremys leprosa* shells and demonstrates their usefulness as non-invasive bioindicators of environmental contamination. Calcium and phosphorus were the dominant elements in the shell matrix, consistent with previous research on chelonian and other vertebrate hard tissues in which Ca–P complexes contribute to structural stability [43]. Significant sex-related differences were detected, with males exhibiting higher concentrations of Mg, Mn, Sb, and Pb, while females showed elevated levels of Al. Such dimorphism aligns with earlier observations in freshwater turtles, where sex, behavioral patterns, and reproductive physiology influenced contaminant burdens [55,67,76].

Micro-XRF elemental mapping provided spatially resolved information that complemented bulk chemical analyses. The observed patterns—uniform distribution of structural mineral elements and heterogeneous hotspots of contaminant metals—highlight the value of turtle shells as non-invasive and integrative bioindicator tissues. This approach strengthens ecological risk assessment by combining quantitative concentration data with spatial

localization, offering a more nuanced perspective for conservation-oriented biomonitoring. Correlations between shell metal concentrations and those in environmental compartments, particularly sediments, confirmed that shells integrate long-term exposure, consistent with patterns documented in other keratinous tissues such as fish scales and turtle eggshells [66,77,78]. The presence and accumulation of toxic elements such as Pb and Sb underscore potential ecological risks for turtle populations inhabiting polluted wetlands and highlight the need for continued monitoring. Importantly, the use of shells as a sampling matrix provides a practical and ethical alternative to invasive tissue collection, aligning with conservation priorities. Collectively, these findings reinforce the growing recognition of freshwater turtles as reliable sentinel species for assessing aquatic ecosystem health [43,55]. Future research that expands spatial and temporal sampling, incorporates biomarkers of physiological stress, and examines trophic transfer pathways will further refine the application of turtle shells in ecological risk assessment and conservation management.

Some metal concentrations in our study, including Cu, Ni, As, and Pb, were frequently below detection limits, a common challenge in ecotoxicology that results in censored data and reduces statistical power [79]. Although our sampling design captured broad patterns of contamination, it may have overlooked fine-scale variation due to limited site coverage and the underrepresentation of juveniles and egg-stage individuals. This limitation reflects a broader trend in freshwater turtle ecotoxicology, as recent reviews have highlighted that most studies lack life-stage diversity and sufficient resolution across habitat gradients [80]. In particular, these reviews emphasized a “significant lack of data” on young turtles and called for non-invasive, life-stage-inclusive monitoring approaches.

Additionally, our study was restricted to a single time point, preventing the assessment of seasonal or long-term trends in contaminant burdens. Without repeated measurements across seasons or years, only a snapshot of exposure can be inferred, leaving episodic events or gradual accumulation undetected. Systematic reviews underline the importance of longitudinal monitoring to better understand temporal dynamics in metal exposure and their impacts on turtle health [81]. Future studies should integrate dietary analyses, physiological biomarkers, and non-invasive long-term sampling to improve our understanding of metal exposure in turtles. For example, stable isotope analysis can clarify habitat use and foraging pathways linked to contamination, while biomarkers such as catalase and superoxide dismutase (SOD) can indicate physiological effects. Non-lethal sampling over extended periods will further enable tracking of exposure trends and support informed conservation management [80,81].

**Author Contributions:** Conceptualization: H.A. and B.B.; Sampling process: B.B., S.C. and A.S.; Methodology: H.M.C. and B.D.; Formal analysis: K.N.; Data curation: K.N. and H.A.; Writing—original draft: H.A.; Writing—review and editing: H.M.C. and Z.V.; Visualization: S.C. and A.S.; Supervision: H.M.C. All authors have read and agreed to the published version of the manuscript.

**Funding:** This research received no external funding.

**Data Availability Statement:** The datasets generated and analyzed during this study are available from the corresponding author upon reasonable request.

**Acknowledgments:** The authors would like to thank the Algerian team for the field assistants and volunteers of the University of Science and Technology Houari Boumediene (USTHB), for their support during turtle sampling and data collection. We also thank Jenő Nagy for organizing the workshop that enabled this fruitful collaboration. Our gratitude extends to Maria Del Pilar Gomez Ramirez and Daniel Escoriza for their support and guidance. We are grateful to the HUN-REN ATOMKI Institute for Nuclear Research, Hungarian Academy of Sciences, for providing access to facilities and technical assistance with elemental analyses. The measurements at ATOMKI were supported by the GINOP-2.3.3-15-2016-00029 “HSLab” project.

**Conflicts of Interest:** The authors declare no conflicts of interest.

## References

1. Malaj, E.; Von der Ohe, P.C.; Grote, M.; Kühne, R.; Mondy, C.P.; Usseglio-Polatera, P.; Brack, W.; Schäfer, R.B. Organic chemicals jeopardize the health of freshwater ecosystems on the continental scale. *Proc. Natl. Acad. Sci. USA* **2014**, *111*, 9549–9554. [CrossRef]
2. Ali, H.; Khan, E.; Sajad, M.A. Phytoremediation of heavy metals—Concepts and applications. *Chemosphere* **2013**, *91*, 869–881. [CrossRef]
3. Hashem, M.A.; Nur-A-Tomal, M.S.; Mondal, N.R.; Rahman, M.A. Hair burning and liming in tanneries is a source of pollution by arsenic, lead, zinc, manganese and iron. *Environ. Chem. Lett.* **2017**, *15*, 501–506. [CrossRef]
4. Aib, H.; Czedli, H.; Baranyai, E.; Sajtos, Z.; Dönczö, B.; Parvez, M.S.; Berta, C.; Varga, Z.; Benhizia, R.; Nyeste, K. Fish Scales as a Non-Invasive Method for Monitoring Trace and Macroelement Pollution. *Biology* **2025**, *14*, 344. [CrossRef] [PubMed]
5. Ebol, E.L.; Donoso, C.H.; Saura, R.B.D.; Ferol, R.J.C.; Mozar, J.R.D.; Bermon, A.N.; Manongas, J.; Libot, J.C.H.; Matabilas, C.J.; Jumawan, J.C.; et al. Heavy Metals Accumulation in Surface Waters, Bottom Sediments and Aquatic Organisms in Lake Mainit, Philippines. *Int. Lett. Nat. Sci.* **2020**, *79*, 40–49. [CrossRef]
6. Jaishankar, M.; Tseten, T.; Anbalagan, N.; Mathew, B.B.; Beeregowda Toxicity, K.N. mechanism and health effects of some heavy metals. *Interdiscip. Toxicol.* **2014**, *7*, 60–72. [CrossRef]
7. Mahboob, S.; Al-Balwai, H.F.A.; Al-Misned, F.; Al-Ghanim, K.A.; Ahmad, Z. A study on the accumulation of nine heavy metals in some important fish species from a natural reservoir in Riyadh, Saudi Arabia. *Toxicol. Environ. Chem.* **2014**, *96*, 783–798. [CrossRef]
8. Csuros, M.; Csuros, C. *Environmental Sampling and Analysis for Metals*; CRC Press: Boca Raton, FL, USA, 2016; pp. 1–372. [CrossRef]
9. Duffus, J.H. ‘Heavy metals’—A meaningless term? (IUPAC technical report). *Pure Appl. Chem.* **2002**, *74*, 793–807. [CrossRef]
10. Ali, H.; Khan, E. What are heavy metals? Long-standing controversy over the scientific use of the term ‘heavy ‘metals’—proposal of a comprehensive definition. *Toxicol. Environ. Chem.* **2018**, *100*, 6–19. [CrossRef]
11. Alloway, B.J. Heavy Metals in Soils “Trace Metals and Metalloids in Soils and their Bioavailability”. In *Environmental Pollution*; Springer: Dordrecht, The Netherlands, 2013; Volume 22. [CrossRef]
12. Förstner, U.; Wittmann, G.T.W. *Metal Pollution in the Aquatic Environment*; Springer Nature: Durham, NC, USA, 1981. [CrossRef]
13. MacFarlane, G.R.; Burchett, M.D. Cellular distribution of copper, lead and zinc in the grey mangrove, *Avicennia marina* (Forsk.) Vierh. *Aquat. Bot.* **2000**, *68*, 45–59. [CrossRef]
14. Baby, J.; Raj, J.S.; Biby, E.T.; Sankarganesh, P.; Jeevitha, M.V.; Ajisha, S.U.; Rajan, S.S. Toxic effect of heavy metals on aquatic environment. *Int. J. Biol. Chem. Sci.* **2010**, *4*, 62976. [CrossRef]
15. Jiwan, S.; Ajay, K. Effects of Heavy Metals on Soil, Plants, Human Health and Aquatic Life. *Int. J. Res. Chem. Environ.* **2011**, *1*, 15–21.
16. Khan, S.; Hesham, A.E.L.; Qiao, M.; Rehman, S.; He, J.Z. Effects of Cd and Pb on soil microbial community structure and activities. *Environ. Sci. Pollut. Res.* **2010**, *17*, 288–296. [CrossRef] [PubMed]
17. Li, Q.S.; Cai, S.S.; Mo, C.H.; Chu, B.; Peng, L.H.; Yang, F.B. Toxic effects of heavy metals and their accumulation in vegetables grown in a saline soil. *Ecotoxicol. Environ. Saf.* **2010**, *73*, 84–88. [CrossRef]
18. Luo, C.; Liu, C.; Wang, Y.; Liu, X.; Li, F.; Zhang, G.; Li, X. Heavy metal contamination in soils and vegetables near an e-waste processing site, south China. *J. Hazard. Mater.* **2011**, *186*, 481–490. [CrossRef]
19. Zaynab, M.; Al-Yahyai, R.; Ameen, A.; Sharif, Y.; Ali, L.; Fatima, M.; Khan, K.A.; Li, S. Health and environmental effects of heavy metals. *J. King Saud. Univ. Sci.* **2022**, *34*, 101653. [CrossRef]
20. Mitra, S.; Chakraborty, A.J.; Tareq, A.M.; Emran, T.B.; Nainu, F.; Khushro, A.; Idris, A.M.; Khandaker, M.U.; Osman, H.; Alhumaydhi, F.A.; et al. Impact of heavy metals on the environment and human health: Novel therapeutic insights to counter the toxicity. *J. King Saud. Univ. Sci.* **2022**, *34*, 101865. [CrossRef]
21. Ali, H.; Khan, E.; Ilahi, I. Environmental Chemistry and Ecotoxicology of Hazardous Heavy Metals: Environmental Persistence, Toxicity, and Bioaccumulation. *J. Chem.* **2019**, *2019*, 6730305. [CrossRef]
22. Bouhezila, F.; Hacene, H. Water quality assessment in Réghaïa (North of Algeria) lake basin by using traditional approach and water quality indices. *Kuwait J. Sci.* **2020**, *47*, 57–71.
23. Network, M.M. Lake Réghaïa—The MedWet Managers Network. Available online: <https://medwetmanagers.net/marine-and-coastal-wetlands/reghaia-lake-algeria> (accessed on 5 May 2025).
24. Le Gal, A.S.; Priol, P.; Georges, J.Y.; Verneau, O. Population structure and dynamics of the Mediterranean Pond Turtle *Mauremys leprosa* (Schweigger, 1812) in contrasted polluted aquatic environments. *Environ. Pollut.* **2023**, *330*, 121746. [CrossRef]
25. Luiselli, L. *Mauremys leprosa*, IUCN Red List of Threatened Species, January 2023. Available online: <https://www.iucnredlist.org/species/158468/207995085> (accessed on 5 May 2025).
26. U.S. Fish and Wildlife Service. Mediterranean Turtle (*Mauremys leprosa*). 2023. Available online: [https://commons.wikimedia.org/wiki/File:Mediterranean\\_Pond\\_Turtle](https://commons.wikimedia.org/wiki/File:Mediterranean_Pond_Turtle) (accessed on 13 November 2025).

27. Hassani, M.S.E.L.; El Hassan, E.M.; Slimani, T.; Bonnet, X. Morphological and physiological assessments reveal that freshwater turtle (*Mauremys leprosa*) can flourish under extremely degraded-polluted conditions. *Chemosphere* **2019**, *220*, 432–441. [CrossRef]
28. Sakai, H.; Saeki, K.; Ichihashi, H.; Suganuma, H.; Tanabe, S.; Tatsukawa, R. Species-specific distribution of heavy metals in tissues and organs of loggerhead turtle (*Caretta caretta*) and green turtle (*Chelonia mydas*) from Japanese coastal waters. *Mar. Pollut. Bull.* **2000**, *40*, 701–709. [CrossRef]
29. Nisa, Z.U.; Sultana, S.; Al-Ghanim, K.; Ghazla; Khan, Q.F.; Al-Misned, F.; Atique, U.; Ahmed, Z.; Mahboob, S. Comparative assessment of heavy metal bioaccumulation in skeletal muscles of softshell and hard-shell freshwater turtles. *J. King Saud. Univ. Sci.* **2021**, *33*, 101463. [CrossRef]
30. De Solla, S.R.; Fernie, K.J. Characterization of contaminants in snapping turtles (*Chelydra serpentina*) from Canadian Lake Erie Areas of Concern: St. Clair River, Detroit River, and Wheatley Harbour. *Environ. Pollut.* **2004**, *132*, 101–112. [CrossRef] [PubMed]
31. Burger, J.; Jeitner, C.; Schneider, L.; Vogt, R.; Gochfeld, M. Arsenic; cadmium; chromium; lead; mercury, and selenium levels in blood of four species of turtles from the Amazon in Brazil. *J. Toxicol. Environ. Health-Part A Curr. Issues* **2010**, *73*, 33–40. [CrossRef]
32. Meyers-Schöne, L.; Shugart, L.R.; Walton, B.T.; Beauchamp, J.J. Comparison of two freshwater turtle species as monitors of radionuclide and chemical contamination: DNA Damage and residue analysis. *Environ. Toxicol. Chem.* **1993**, *12*, 1487–1496. [CrossRef]
33. Gahmous, S.A.; Tiar, G.; Tiar-Saadi, M.; Bouslama, Z.; Široký, P. Reproductive Traits Demonstrate How Well the Mediterranean Stripe-Necked Turtle *Mauremys leprosa* Can Flourish under Highly Degraded–Polluted Conditions. *Biology* **2022**, *11*, 1562. [CrossRef]
34. Bakhouch, B.; Ghoullem, T.; Imed, D.; Khalil, D.; Escoriza, D. Phenology and population structure of the mediterranean stripe-necked terrapin *Mauremys leprosa* (Schweigger, 1812) in the Reghaïa Lake (northern Algeria). *Basic Appl. Herpetol.* **2019**, *33*, 43–51. [CrossRef]
35. Cox, N.; Chanson, J.; Stuart, S. *The Status and Distribution of Reptiles and Amphibians of the Mediterranean Basin*; The World Conservation Union (IUCN): Gland, Switzerland, 2006.
36. Salvador, A.; Pleguezuelos, J.M. Reptiles españoles: Identificación, historia natural y distribución. *Ichthyol. Herpetol.* **2003**, *2003*, 201–202. [CrossRef]
37. Djitli, Y.; Boix, D.; Milla, A.; Marniche, F.; Tornero, I.; Cunillera-Montcusí, D.; Sala, J.; Gascón, S.; Quintana, X.D.; Daoudi-Hacini, S. Annual cycle of water quality and macroinvertebrate composition in Algerian wetlands: A case study of lake Réghaïa (Algeria). *Limnetica* **2021**, *40*, 399–415. [CrossRef]
38. Rousseau, R. Detection Limit and Estimate of Uncertainty of Analytical XRF Results. *Rigak J.* **2001**, *18*. Available online: <https://www.scribd.com/document/481280444/Detection-limit-and-estimate-of-uncertainty-of-analytical-XRF-results> (accessed on 27 October 2025).
39. Benjamini, Y.; Hochberg, Y. Controlling the False Discovery Rate: A Practical and Powerful Approach to Multiple Testing. *J. R. Stat. Soc. Ser. B Stat. Methodol.* **1995**, *57*, 289–300. [CrossRef]
40. Rani, N.; Bisht, N.; Chauhan, S.; Singh, D. Exploring the Functionality and Diversity of Biological Materials. In *Mechanics and Materials Science of Biological Materials*; Springer: Singapore, 2025; Volume Part F558; pp. 203–227. [CrossRef]
41. Rothschild, B.M.; Schultze, H.P.; Pellegrini, R. Osseous and Other Hard Tissue Pathologies in Turtles and Abnormalities of Mineral Deposition. In *Morphology and Evolution of Turtles*; Vertebrate Paleobiology and Paleoanthropology; Springer: Dordrecht, The Netherlands, 2013; pp. 501–534. ISBN 9789400743083. [CrossRef]
42. Wu, D.H.; Preskitt, C.; Gresham-Fiegel, C.J.I.B.R. Chemical and Physiological Change from Calcium Carbonate to Calcium Phosphate in Skeletal Structures. *Insights Biomed. Res.* **2021**, *5*, 139–148. [CrossRef]
43. Becker, D.N.; Brown, D.J.; Hubbart, J.A.; Anderson, J.T. Environmental factors influencing bioaccumulation of xenobiotic metals in freshwater turtles. *Environ. Pollut. Bioavailab.* **2025**, *37*, 2474007. [CrossRef]
44. Kausar, J.; Naureen, I. Benefit of Egg Shell as Calcium Source in Egg Production and Bone Development. *Sch. Int. J. Anat. Physiol.* **2021**, *4*, 196–200. [CrossRef]
45. Sinclair-Black, M.; Garcia, R.A.; Ellestad, L.E. Physiological regulation of calcium and phosphorus utilization in laying hens. *Front. Physiol.* **2023**, *14*, 1112499. [CrossRef]
46. Taylor, T.-G. The Role of The Skeleton in Egg-Shell Formation. *Ann. De Biol. Anim. Biochim. Biophys.* **1970**, *10*, 83–91. Available online: <https://hal.science/hal-00896581v1> (accessed on 13 November 2025). [CrossRef]
47. Naghilou, Z.; Rajaei, F.; Behrooz, R.D.; Chakraborty, P. Trace elements in barnacle, egg contents, and egg shells of the critically endangered hawksbill turtle (*Eretmochelys imbricata*) from the Persian Gulf Iran. *Environ. Res.* **2025**, *282*, 122032. [CrossRef]
48. Cox, R.M.; Butler, M.A.; John-Alder, H.B. The evolution of sexual size dimorphism in reptiles. *Sex Size Gen. Roles: Evol. Stud. Sex. Size Dimorphism* **2007**, *5*, 38–49. [CrossRef]
49. Katona, G.; Vági, B.; Végvári, Z.; Liker, A.; Freckleton, R.P.; Bókony, V.; Székely, T. Are evolutionary transitions in sexual size dimorphism related to sex determination in reptiles? *J. Evol. Biol.* **2021**, *34*, 594–603. [CrossRef]

50. Gibbons, J.W.; Lovich, J. Sexual Dimorphism in Turtles with Emphasis on the slider turtle (*Trachemys scripta*). *Herpetol. Monogr.* **1990**, *4*, 1–29. [[CrossRef](#)]
51. Keller, J.M.; McClellan-Green, P.D.; Kucklick, J.R.; Keil, D.E.; Peden-Adams, M.M. Effects of Organochlorine Contaminants on Loggerhead Sea Turtle Immunity: Comparison of a Correlative Field Study and In Vitro Exposure Experiments. *Environ. Health Perspect.* **2006**, *114*, 70–76. [[CrossRef](#)]
52. Hopkins, B.C.; Hopkins, W.A.; Moore, I.T.; Hawley, D.M. *Mercury Bioaccumulation and Adverse Reproductive Effects in Snapping Turtles Inhabiting a Historically Contaminated River*; Virginia Tech: Blacksburg, VA, USA, 2012.
53. Hopkins, B.C.; Willson, J.D.; Hopkins, W.A. Mercury exposure is associated with negative effects on turtle reproduction. *Environ. Sci. Technol.* **2013**, *47*, 2416–2422. [[CrossRef](#)]
54. Stewart, J.R.; Eay, T.W. Patterns of maternal provision and embryonic mobilization of calcium in oviparous and viviparous squamate reptiles. *Herpetol. Conserv. Biol.* **2010**, *5*, 341–359.
55. Bishop, B.E.; Savitzky, B.A.; Abdel-Fattah, T. Lead bioaccumulation in emydid turtles of an urban lake and its relationship to shell disease. *Ecotoxicol. Environ. Saf.* **2010**, *73*, 565–571. [[CrossRef](#)]
56. Maccolini, É. Nutrition for Aquatic Turtles. Vet et Nous. 2024. Available online: <https://www.vetetnous.com/en/tips/nutrition-for-aquatic-turtles/> (accessed on 18 September 2025).
57. Wilczek, G.; Babczyńska, A.; Wilczek, P. Antioxidative responses in females and males of the spider *Xerolycosa nemoralis* (Lycosidae) exposed to natural and anthropogenic stressors. *Comp. Biochem. Physiol. Part C Toxicol. Pharmacol.* **2013**, *157*, 119–131. [[CrossRef](#)] [[PubMed](#)]
58. Wilczek, G.; Rost-Roszkowska, M.; Wilczek, P.; Babczyńska, A.; Szulińska, E.; Sonakowska, L.; Marek-Swedzioł, M. Apoptotic and necrotic changes in the midgut glands of the wolf spider *Xerolycosa nemoralis* (Lycosidae) in response to starvation and dimethoate exposure. *Ecotoxicol. Environ. Saf.* **2014**, *101*, 157–167. [[CrossRef](#)] [[PubMed](#)]
59. Sparling, D.W.; Linder, G.; Bishop, C.A.; Krest, S.K. Ecotoxicology of Amphibians and Reptiles. In *Ecotoxicology of Amphibians and Reptiles*, 2nd ed.; CRC Press: Boca Raton, FL, USA, 2010; pp. 1–946. [[CrossRef](#)]
60. Martínez-López, E.; Gómez-Ramírez, P.; Espín, S.; Aldeguer, M.P.; García-Fernández, A.J. Influence of a Former Mining Area in the Heavy Metals Concentrations in Blood of Free-Living Mediterranean Pond Turtles (*Mauremys leprosa*). *Bull. Environ. Contam. Toxicol.* **2017**, *99*, 167–172. [[CrossRef](#)]
61. Parolini, M.; Sturini, M.; Maraschi, F.; Profumo, A.; Costanzo, A.; Caprioli, M.; Rubolini, D.; Ambrosini, R.; Canova, L. Trace elements fingerprint of feathers differs between breeding and non-breeding areas in an Afro-Palaearctic migratory bird, the barn swallow (*Hirundo rustica*). *Environ. Sci. Pollut. Res. Int.* **2020**, *28*, 15828. [[CrossRef](#)]
62. Pushie, M.J.; Pickering, I.J.; Korbas, M.; Hackett, M.J.; George, G.N. Elemental and Chemically Specific X-ray Fluorescence Imaging of Biological Systems. *Chem. Rev.* **2014**, *114*, 8499–8541. [[CrossRef](#)]
63. Pushie, M.J.; Sylvain, N.J.; Hou, H.; Hackett, M.J.; Kelly, M.E.; Webb, S.M. X-ray fluorescence microscopy methods for biological tissues. *Metallomics* **2022**, *14*, mfac032. [[CrossRef](#)]
64. Jian, L.; Zhang, T.; Lin, L.; Xiong, J.; Shi, H.; Wang, J. Transfer and accumulation of trace elements in seawater, sediments, green turtle forage, and eggshells in the Xisha Islands, South China Sea. *Environ. Sci. Pollut. Res.* **2022**, *29*, 50832–50844. [[CrossRef](#)]
65. Wilkinson, A.; Ariel, E.; van de Merwe, J.; Brodie, J. Green Turtle (*Chelonia mydas*) Blood and Scute Trace Element Concentrations in the Northern Great Barrier Reef. *Environ. Toxicol. Chem.* **2023**, *42*, 2375–2388. [[CrossRef](#)]
66. Jian, L.; Guo, R.; Zheng, X.; Shi, H.; Wang, J. Trace elements in green turtle eggshells and coral sand sediments from the Xisha Islands, South China Sea. *Mar. Pollut. Bull.* **2021**, *164*, 112036. [[CrossRef](#)] [[PubMed](#)]
67. Adel, M.; Cortés-Gómez, A.A.; Dadar, M.; Riyahi, H.; Girondot, M. A comparative study of inorganic elements in the blood of male and female Caspian pond turtles (*Mauremys caspica*) from the southern basin of the Caspian Sea. *Environ. Sci. Pollut. Res.* **2017**, *24*, 24965–24979. [[CrossRef](#)] [[PubMed](#)]
68. Pounds, J.G. Effect of lead intoxication on calcium homeostasis and calcium-mediated cell function: A review. *Neurotoxicology* **1984**, *5*, 295–331.
69. Al-Rawahy, S.H. Accumulation of metals in the egg yolk and liver of hatchling of green turtles *Chelonia mydas* at Ras Al Hadd, Sultante of Oman. *J. Biol. Sci.* **2007**, *7*, 925–930. [[CrossRef](#)]
70. Santhosh, K.; Kamala, K.; Ramasamy, P.; Musthafa, M.S.; Almujri, S.S.; Asdaq, S.M.B.; Sivaperumal, P. Unveiling the silent threat: Heavy metal toxicity devastating impact on aquatic organisms and DNA damage. *Mar. Pollut. Bull.* **2024**, *200*, 116139. [[CrossRef](#)]
71. Steinhardt, J.; Butler, P.G.; Carroll, M.L.; Hartley, J. The application of long-lived bivalve sclerochronology in environmental baseline monitoring. *Front. Mar. Sci.* **2016**, *3*, 176. [[CrossRef](#)]
72. Collin, S.; Baskar, A.; Geevarghese, D.M.; Ali, M.N.V.S.; Bahubali, P.; Choudhary, R.; Lvov, V.; Tovar, G.I.; Senatov, F.; Koppala, S.; et al. Bioaccumulation of lead (Pb) and its effects in plants: A review. *J. Hazard. Mater. Lett.* **2022**, *3*, 100064. [[CrossRef](#)]
73. Kumar, A.; Kumar, A.; Cabral-Pinto, M.; Chaturvedi, A.K.; Shabnam, A.A.; Subrahmanyam, G.; Mondal, R.; Gupta, D.K.; Malyan, S.K.; Kumar, S.S.; et al. Lead Toxicity: Health Hazards, Influence on Food Chain, and Sustainable Remediation Approaches. *Int. J. Environ. Res. Public Health* **2020**, *17*, 2179. [[CrossRef](#)]

74. Wang, L.; Yin, Z.; Yan, W.; Hao, J.; Tian, F.; Shi, J. Nitrate-dependent antimony oxidase in an uncultured Symbiobacteriaceae member. *ISME J.* **2024**, *18*, wrae204. [[CrossRef](#)]
75. Zhong, Q.; Li, L.; He, M.; Ouyang, W.; Lin, C.; Liu, X. Toxicity and bioavailability of antimony to the earthworm (*Eisenia fetida*) in different agricultural soils. *Environ. Pollut.* **2021**, *291*, 118215. [[CrossRef](#)]
76. Ibáñez, A.; Martínez-Silvestre, A.; Podkowa, D.; Woźniakiewicz, A.; Woźniakiewicz, M.; Pabijan, M. The chemistry and histology of sexually dimorphic mental glands in the freshwater turtle, *Mauremys leprosa*. *PeerJ* **2020**, *2020*, e9047. [[CrossRef](#)] [[PubMed](#)]
77. Chenet, T.; Schwarz, G.; Neff, C.; Hattendorf, B.; Günther, D.; Martucci, A.; Cescon, M.; Baldi, A.; Pasti, L. Scallop shells as biosorbents for water remediation from heavy metals: Contributions and mechanism of shell components in the adsorption of cadmium from aqueous matrix. *Heliyon* **2024**, *10*, e29296. [[CrossRef](#)] [[PubMed](#)]
78. Rahman, S.A.; Abdullah, N.A.; Chowdhury, A.J.K.; Yunus, K. Fish Scales as a Bioindicator of Potential Marine Pollutants and Carcinogens in Asian Sea Bass and Red Tilapia within the Coastal Waters of Pahang, Malaysia. *J. Coast. Res.* **2018**, *82*, 120–125. [[CrossRef](#)]
79. Salvat-Leal, I.; Cortés-Gómez, A.A.; Romero, D.; Girondot, M. New Method for Imputation of Unquantifiable Values Using Bayesian Statistics for a Mixture of Censored or Truncated Distributions: Application to Trace Elements Measured in Blood of Olive Ridley Sea Turtles from Mexico. *Animals* **2022**, *12*, 2919. [[CrossRef](#)]
80. Hopkins, W.A.; Bodinof, C.; Budischak, S.; Perkins, C. Nondestructive indices of mercury exposure in three species of turtles occupying different trophic niches downstream from a former chloralkali facility. *Ecotoxicology* **2013**, *22*, 22–32. [[CrossRef](#)]
81. Héritier, L.; Meistertzheim, A.L.; Verneau, O. Oxidative stress biomarkers in the Mediterranean pond turtle (*Mauremys leprosa*) reveal contrasted aquatic environments in Southern France. *Chemosphere* **2017**, *183*, 332–338. [[CrossRef](#)]

**Disclaimer/Publisher’s Note:** The statements, opinions and data contained in all publications are solely those of the individual author(s) and contributor(s) and not of MDPI and/or the editor(s). MDPI and/or the editor(s) disclaim responsibility for any injury to people or property resulting from any ideas, methods, instructions or products referred to in the content.